

# Ad Recommendation in a Collapsed and Entangled World

Junwei Pan, Wei Xue, Ximei Wang, Haibin Yu,  
Xun Liu, Shijie Quan, Xueming Qiu, Dapeng Liu, Lei Xiao, Jie Jiang  
{jonaspan, weixue, messixmwang, nathanhbyu}@tencent.com  
Tencent Inc.  
China

## ABSTRACT

In this paper, we present an industry ad recommendation system, paying attention to the challenges and practices of learning appropriate representations. Our study begins by showcasing our approaches to preserving priors when encoding features of diverse types into embedding representations. Specifically, we address sequence features, numeric features, pre-trained embedding features, as well as sparse ID features. Moreover, we delve into two pivotal challenges associated with feature representation: the *dimensional collapse* of embeddings and the *interest entanglement* across various tasks or scenarios. Subsequently, we propose several practical approaches to effectively tackle these two challenges. We then explore several training techniques to facilitate model optimization, reduce bias, and enhance exploration. Furthermore, we introduce three analysis tools that enable us to comprehensively study feature correlation, dimensional collapse, and interest entanglement. This work builds upon the continuous efforts of Tencent's ads recommendation team in the last decade. It not only summarizes general design principles but also presents a series of off-the-shelf solutions and analysis tools. The reported performance is based on our online advertising platform, which handles hundreds of billions of requests daily, serving millions of ads to billions of users.

## KEYWORDS

Recommendation Systems, Representation Learning, Dimensional Collapse, Disentanglement

### ACM Reference Format:

Junwei Pan, Wei Xue, Ximei Wang, Haibin Yu., Xun Liu, Shijie Quan, Xueming Qiu, Dapeng Liu, Lei Xiao, Jie Jiang. 2018. Ad Recommendation in a Collapsed and Entangled World. In *Proceedings of Make sure to enter the correct conference title from your rights confirmation email (Conference acronym 'XX)*. ACM, New York, NY, USA, 11 pages. <https://doi.org/XXXXXXX.XXXXXXX>

## 1 INTRODUCTION

The online advertising industry, valued in the billions of dollars, stands as a remarkable testament to the successful application of machine learning. Various advertising formats, including sponsored search advertising, contextual advertising, display advertising, and real-time bidding auctions, heavily rely on the accurate,

rapid, and reliable prediction of ad click-through or conversion rates by learned models.

In the past decade, deep learning has achieved remarkable success across various domains, including computer vision (CV) [23, 31], natural language processing (NLP) [1, 15, 55], and recommender systems [36, 67]. The efficacy of deep learning heavily relies on the selection of appropriate data representations [3, 60, 61]. In CV and NLP, researchers have extensively investigated various aspects of representation learning, such as priors [55], smoothness and curse of dimensionality [5], depth and abstraction [4], disentangling factors of variations [61] and uniformity of representations [26, 27].

In the realm of recommendation systems, there are also many representation-oriented works which explore techniques to handle various types of features [9, 19, 29, 69, 71], capture feature correlations through explicit or implicit feature interactions [12, 20, 34, 38, 44, 53, 59], address the entangled interest within users' complex behaviors [62], particularly in multi-task [37, 52] or multi-scenario [7, 47, 73] settings, and enhance data representation through self-supervised learning [56, 74]. However, several fundamental questions regarding representation learning in large-scale real-world ad recommenders remain unanswered:

- *Priors for Representation*: Real-world systems encompass various types of features from diverse sources, including sequence features (e.g., user click/conversion history), numeric features (e.g., semantic-preserving ad IDs), and embedding features from pre-trained external models. Preserving the inherent priors of these features while encoding them in recommendation systems is crucial.
- *Dimensional Collapse*: The encoding process maps all features into embeddings, typically represented as  $K$ -dimensional vectors, which are learned during model training. However, we observe that the embeddings of many fields tend to occupy a lower-dimensional subspace instead of fully utilizing the available  $K$ -dimensional space. Such dimensional collapse not only leads to parameter wastage but also limits the scalability of recommendation models.
- *Interest Entanglement*: User responses in ad recommender systems are influenced by complex interest among various factors, particularly when multiple tasks or scenarios are learned simultaneously. Existing shared-embedding approaches fail to disentangle these factors adequately, as they rely on a single entangled embedding for each feature.

Our paper will be organized as follows. We'll present an overview of our model architecture in Section 2. In Section 3, we demonstrate the encoding techniques employed to incorporate the temporal, ordinal, or distance priors of different feature types into the representation. In Section 4, we delve into the root causes of the embedding dimensional collapse and propose several approaches to address

Permission to make digital or hard copies of all or part of this work for personal or classroom use is granted without fee provided that copies are not made or distributed for profit or commercial advantage and that copies bear this notice and the full citation on the first page. Copyrights for components of this work owned by others than the author(s) must be honored. Abstracting with credit is permitted. To copy otherwise, to republish, to post on servers or to redistribute to lists, requires prior specific permission and/or a fee. Request permissions from [permissions@acm.org](mailto:permissions@acm.org).  
Conference acronym 'XX, June 03–05, 2018, Woodstock, NY

© 2018 Copyright held by the owner/author(s). Publication rights licensed to ACM.  
ACM ISBN 978-1-4503-XXXX-X/18/06...\$15.00  
<https://doi.org/XXXXXXX.XXXXXXX>

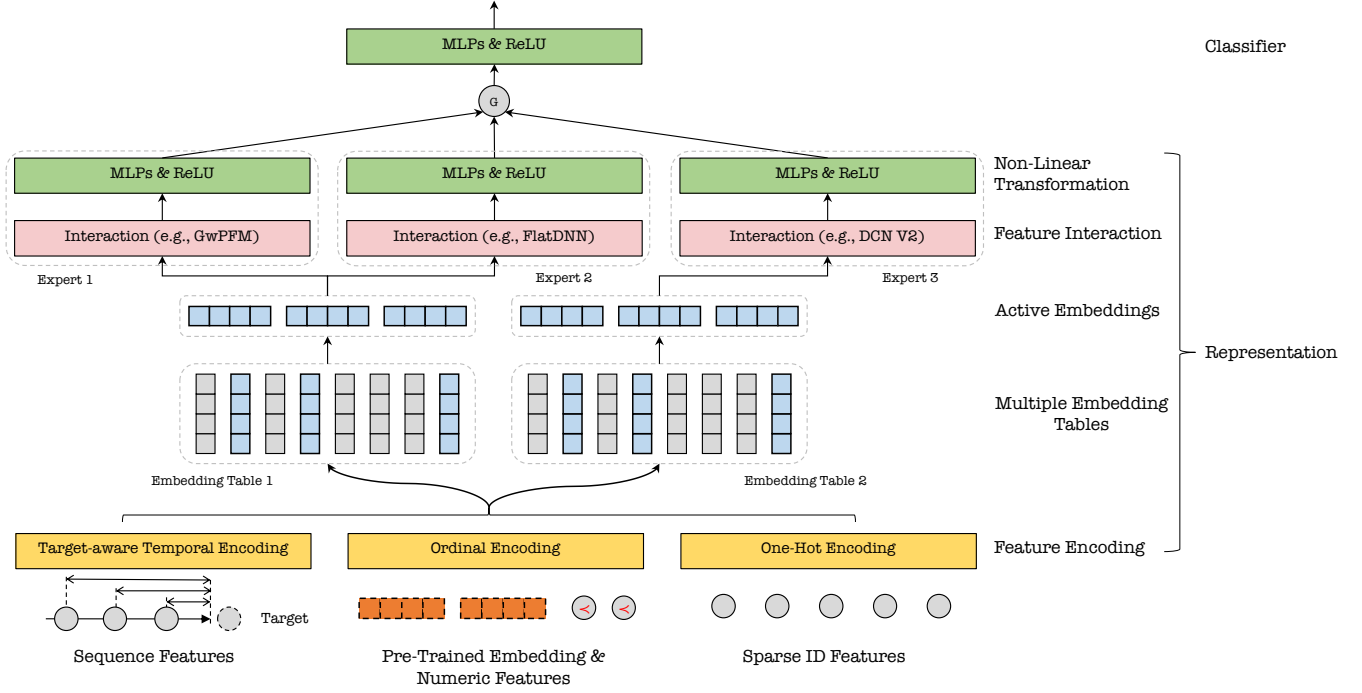


**Figure 1: Overall model architecture for single-task learning.** Features of various types are first encoded by corresponding methods. Then multiple embeddings are looked up for each encoded ID from multiple independent embedding tables. Multiple heterogeneous experts interact embeddings with each other from the same embedding table, followed by non-linear transformations and the final classifier.

this issue. Section 5 focuses on the discussion of interest entanglement across various tasks or scenarios. In Section 6, we present various model training techniques. Finally, we present a set of off-the-shelf tools in Section 7 that facilitate the analysis of feature correlations, dimensional collapse, and interest entanglement.

## 2 BRIEF SYSTEM OVERVIEW

The overall architecture of our ad recommendation model for single-task learning is depicted in Fig. 1 (Refer to Fig. 4 for multi-task learning model architecture). We have adopted a widely employed Embedding & Explicit Interaction framework [36, 67], comprising four key modules: feature encoding, multi-embedding lookup, experts (feature interactions and MLPs), and classification towers. In the feature encoding module, all features undergo encoding methods tailored to their respective types. Subsequently, based on the resulting encoded IDs, multiple embeddings are retrieved from several individual embedding tables for each feature. Embeddings from the same table are then explicitly interacted with one another within the expert module, followed by Multi-Layer Perceptrons (MLPs) with non-linear transformation. The classification towers receive the gate-weighted sum of the experts' outputs. The sigmoid activation function is applied to generate the final prediction.

For single-task learning, such as Click-Through Rate (CTR) prediction, a single tower is employed as shown Fig. 1. Conversely, for multi-task learning (MTL), such as Conversion Rate (CVR) prediction where each conversion type is treated as an individual task, multiple towers and corresponding gates are utilized, with each

tower dedicated to a specific group of conversion types. We need to further evolve the model architecture to resolve the interest entanglement issue in MTL, refer to Fig. 4 for details.

Our team is responsible for ad recommendation across all modules, including retrieval and pre-ranking, CTR prediction (pCTR), (shallow) conversion prediction (pCVR) of various conversion types, deep conversion prediction (pDCVR), and Long-time Value prediction (pLTV). There are lots of commonalities regarding the model design principle among these modules, and we mainly discuss the pCTR and pCVR as representative modules of single-task and multi-task learning, respectively. Our models serve various scenarios within Tencent, encompassing Moments (social stream), Channels (micro-video stream), Official Accounts (subscription), Tencent News, Tencent Video (long-video platform), as well as DSP (Demand Side Platform).

## 3 FEATURE ENCODING

In industrial ad recommendation systems, features are generated from many sources, belonging to different types, such as sequence, numeric and embedding features. When encoding these features, we'd like to preserve their inherent temporal, ordinal, or distance priors as much as possible. For sparse ID features, we simply take a one-hot encoding.

### 3.1 Sequence Features

A user's history behaviors reflect her interest, making them critical in recommendations. One key characteristic of such features is that

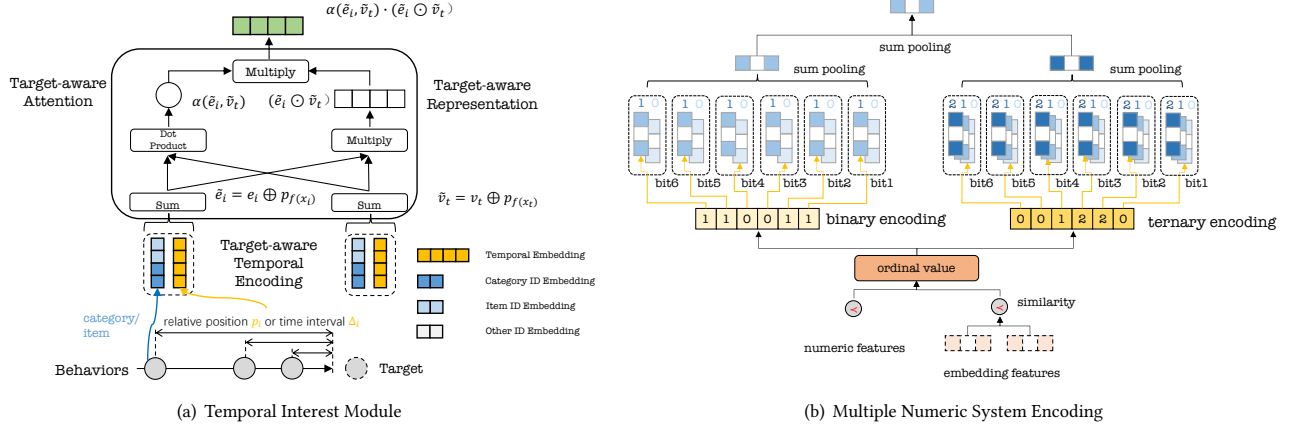


**Figure 2: Illustration of temporal interest module (TIM) for sequence features and multiple numeral systems (MNS) encoding for numeric and pre-trained embedding features.**

there are strong semantic as well as temporal correlations between these behaviors and the target [72]. For example, given a target, those behaviors that are either semantically related (e.g., belonging to the same category with target ad) or temporally close are more informative to predict the user’s response.

We propose Temporal Interest Module (TIM) [72] to learn the above-mentioned four-way semantic-temporal correlation between quadruplet (behavior semantic, target semantic, behavior temporal, target temporal). Specifically, in addition to the semantic encoding, TIM leverages Target-aware Temporal Encoding (TTE) for each behavior, e.g., the *relative position* or *time interval* between each behavior and target. Furthermore, to capture the *quadruple correlation*, TIM employs Target-aware Attention (TA) together with Target-aware Representation (TR) to interact behaviors with the target in both attention and representation, resulting in *explicit 4-way interaction*. Mathematically, the encoding of user behavior sequence  $\mathcal{H}$  can be formulated as:

$$\mathbf{u}_{\text{TIM}} = \sum_{X_i \in \mathcal{H}} \alpha(\tilde{\mathbf{e}}_i, \tilde{\mathbf{v}}_t) \cdot (\tilde{\mathbf{e}}_i \odot \tilde{\mathbf{v}}_t), \quad (1)$$

where  $\alpha(\tilde{\mathbf{e}}_i, \tilde{\mathbf{v}}_t)$  denotes target-aware attention,  $(\tilde{\mathbf{e}}_i \odot \tilde{\mathbf{v}}_t)$  denotes target-aware representation, and  $\tilde{\mathbf{e}}_i = \mathbf{e}_i \oplus \mathbf{p}_{f(X_i)}$  denotes the temporally encoded embedding of the  $i$ -th behavior, which is an element-wise summation of semantic embedding  $\mathbf{e}_i$  and target-aware temporal encoding  $\mathbf{p}_{f(X_i)}$ , which is either the embedding of the relative position of each behavior regarding the target, or the discretized time interval.

**Deployment Details.** In practice, we adopt both relative position and time interval for temporal encoding. The output of TIM is concatenated with the output of the feature interaction module, e.g., GwPFM (will be discussed later), or DCN V2. We apply TIM on the user’s click/conversion category sequence features in various click and conversion prediction tasks across multiple scenarios. TIM brings 1.93% GMV lift in WeChat pCTR, as well as 2.45% GMV and 12.22% GMV(ROI) lift in Game and e-Commerce pLTV.

### 3.2 Numeric Features

Different from the widely-used categorical features, there is inherent partial order between numeric/ordinal features, such as  $\text{Age}_{20} < \text{Age}_{30}$ . To preserve these partial priors, inspired by the  $n$ -ary encoding [9], we propose a simple yet efficient variant, namely Multiple Numeral System (MNS). MNS encodes numeric features by discretizing the numeric values via a numeral system (i.e., binary), and then assign learnable embeddings to the discretization results.

In particular, we employ multiple numeral systems (i.e., binary, ternary, decimal) to tackle the carry and modulo-congruence issue caused by using only one system [9]. For example, a feature value "51" is transformed into code "{6\_1, 5\_1, 4\_0, 3\_0, 2\_1, 1\_1}" according to binary system, and "{6\_0, 5\_0, 4\_1, 3\_2, 2\_2, 1\_0}" according to ternary system. All codes are projected to embeddings and then sum pooled to get the final encoding result. We remove the inter- and intra-attention in the original  $n$ -ary [9] to improve computation efficiency. Formally,

$$\mathbf{f}_{\text{MNS}}(\cdot) = \sum_{k=1}^{K_2} \mathbf{X}_{2k+\mathbb{B}_k} + \sum_{k=1}^{K_3} \mathbf{X}_{3k+\mathbb{C}_k} + \dots + \sum_{k=1}^{K_n} \mathbf{X}_{nk+\mathbb{N}_k} \quad (2)$$

$$\mathbb{B} = \text{func\_binary}(v), \mathbb{C} = \text{func\_ternary}(v), \dots$$

where  $K_2$  and  $K_3$  are the lengths of the encoding list for binary and ternary systems respectively,  $\text{func\_binary}$  and  $\text{func\_ternary}$  are the binarization and ternarization functions respectively.

**Deployment Details.** In an advertising system, ads are often indexed by discrete identifiers (Ad IDs), which are self-incremental IDs and hence meaningless. However, each ad is associated with a creative, which contains abundant visual semantics. Consequently, we replace the Ad IDs by a novel HashID to preserve the visual semantics. Specifically, we first get visual embeddings of ads from a vision model based on their creatives, then apply hashing algorithms such as Locality-Sensitive Hashing (LSH)[57] on them to preserve the visual distances, and finally attain the HashIDs. In this way, ads with similar appearance have contiguous HashIDs, i.e., the hamming distance between the hash coding lists of two similar ads

will be smaller than that of two dissimilar ads. Therefore, HashIDs can be regarded as special numeric features, and we further apply MNS to them to preserve their ordinal priors. Replacing the original self-incremental ad IDs with HashIDs leads to a 1.13% GMV lift in Moments pCVR. In particular, the GMV lift in new ads is much larger (1.74%), where ad IDs cannot be fully learned for new ads due to the lack of feedback. Further, the inconsistency of prediction scores among creatives with identical ads shown to the same user is greatly reduced from 2.44% to 0.30%.

### 3.3 Embedding Features

Besides the main recommendation model, we may train a separate model, such as LLM or GNN, to learn embeddings for entities (users or items). Such embeddings capture the relationship between users and items from a different perspective, *e.g.*, as a Graph or Self-Supervised Language Model, and hence should provide extra information to the recommendation models. The key challenge in leveraging such pre-trained embedding directly in our recommendation system is the semantic gap. That is, these embedding captures different semantics from the collaborative semantics of the ID embeddings in recommendation models [33, 69]. For example, LLM embeddings learn a language semantic, whilst GNN embeddings learn a graph semantic, using a cosine distance [22] rather than inner product distance in matrix factorization-based recommenders.

To mitigate such a semantic gap, we adopt a two-phase approach. Take an external GNN for example. Once we train a GNN model and get the pre-trained embeddings  $\mathbf{v}_u, \mathbf{v}_i$  for each user and item, we first calculate the distance:  $\bar{\mathbf{v}}_u, \bar{\mathbf{v}}_i$ , using the corresponding distance, *i.e.*, cosine in GraphSage [22]. Formally, such a similarity score

$$w_{\text{sim}} = \text{sim}(\bar{\mathbf{v}}_u, \bar{\mathbf{v}}_i) \quad (3)$$

is an ordinal value, and hence similar to numeric features, we can use multiple numeral system encoding as shown in Eq. 2 to transform it into a learnable embedding  $\mathbf{e}_{\text{sim}} = f_{\text{MNS}}(w_{\text{sim}})$ . After that, the encoded embedding is co-trained with the other ID embeddings simultaneously. Thus, the distance priors in the original space are retained, while the co-training of encoding embeddings with ID embeddings aligns them into the same collaborative space.

*Deployment Details.* We employ self-supervised pre-training using GraphSage [22] on a user-ad/content bipartite graph, with clicks in both ad and content recommendation domains as the edges. We encode the cosine similarity between pre-trained user and item embeddings via multiple numeral system encoding and concatenate the resulting representation with that of the feature interaction layer. GNN embeddings are successfully deployed in many scenarios, leading to +1.21%, +0.59%, and 1.47% GMV lift on Moments, Channel, and Applet pCTR.

## 4 TACKLING DIMENSIONAL COLLAPSE

After encoding, all features are transformed into embeddings and then interact with each other explicitly [20, 28, 30, 34, 42, 44, 45, 51, 59]. However, one key side effect of explicit feature interaction is that some dimensions of embeddings collapse. In this section,

we'll first explain dimensional collapse, and then present two different multi-embedding approaches and a collapse-resilient feature interaction function to mitigate it.

### 4.1 Embedding Dimensional Collapse

Recent work [1, 17, 68] has demonstrated that large-scale models especially transformer-based models with billions, even trillions, of parameters can achieve remarkable performance (*e.g.*, GPT-4 [1], LLaMA [54]). Inspired by these works, we explore how to scale up ad recommendation models. Usually, embeddings dominate the number of model parameters, for example, more than 99.99% of parameters in our production model are from embedding of features, such as user ID (at billions level in Tencent), ads, or creative ID (at tens of millions level). Therefore, we start to scale up our model by enlarging the embedding size  $K$ , *e.g.*, increasing  $K$  from 64 to 192. However, it doesn't bring significant performance lift, and sometimes even leads to performance deterioration.

We investigate the learned embedding matrix of each field by singular spectral analysis [27], and observe dimensional collapse. That is, many singular values are very small, indicating that embeddings of many fields end up spanning a lower-dimensional subspace instead of the entire available embedding space [21, 26]. The dimensional collapse of embeddings results in a vast waste of model capacity since many embedding elements are collapsed and hence meaningless. Furthermore, the fact that many embeddings have already collapsed makes it infeasible to scale up models by simply increasing dimension size [2, 21]. Please refer to Sec. 7.2 for details.

We study the root cause of the dimensional collapse and find it's due to the explicit feature interaction module, namely, fields with collapsed dimension (due to various reasons, for example, low cardinality) that make the embeddings of other fields collapse along some dimensions. For example, some fields such as Gender have very low cardinality  $N_{\text{Gen}}$ , making their embeddings only able to span a  $N_{\text{Gen}}$ -dimension space. As  $N_{\text{Gen}}$  is much smaller than embedding size  $K$ , the interaction between these low-dimension embeddings and the possibly high-dimensional embedding (in  $K$ -dimensional) of remaining fields make the latter collapse to an  $N_{\text{Gen}}$ -dimensional subspace.

### 4.2 Multi-Embedding Paradigm

We propose a *multi-embedding paradigm* [21] to mitigate embedding dimensional collapse when scaling up ads recommenders. Specifically, we *scale up the number of embedding tables* instead of the embedding size and incorporate embedding-table-specific feature interaction modules. Given a feature, we look up several embeddings for it, each from a different embedding table. Then all feature embeddings from the same embedding table interact with each other in the corresponding feature interaction module.

One requirement of multi-embedding is that there should be non-linearities such as ReLU after feature interaction; otherwise, the model is equivalent to single-embedding and hence does not capture different patterns. As a solution, we add a non-linear projection after interaction for the model with linear interaction layers. An overall architecture of the multi-embedding paradigm is shown in Figure 1. The multi-embedding paradigm mitigates dimension collapse significantly, since it learns more diverse embeddings in

each sub-space [21]. With multi-embedding paradigm, we achieve *parameter scaling for recommendation models* which has been regarded a great challenge [2]: the model performance improves along with the increase of parameters.

**Deployment Details.** Almost all pCTR models in our platform adopt a Multi-Embedding paradigm. Specifically, we learn multiple different feature interaction experts, e.g., GwPFM (a variant of FFM, which will be described below), IPNN, DCN V2, or FlatDNN, and multiple embedding tables. One or several experts share one of the embedding tables. We name such architecture *Heterogeneous Experts with Multi-Embedding*. For example, the Moments pCTR model consists of a GwPFM, IPNN [44], and FlatDNN, along with two embedding tables. GwPFM and FlatDNN share the first table, while IPNN uses the second one. Switching from a single embedding to the above architecture brings a 3.9% GMV lift in Moments pCTR.

### 4.3 GwPFM: Yet Another Simplified Approach to Multi-Embedding Paradigm

FFM [28] can also be regarded as another approach of the Multi-Embedding paradigm in the sense that FFM also learns multiple embeddings for each feature. In particular, for a dataset with  $M$  fields, FFM learns  $M - 1$  embeddings  $\{v_{i,F_l} | F_l \neq F(i)\}$  for each feature  $x_i$ . When interacting feature  $x_i$  with another feature  $j$ , among  $x_i$ 's embeddings, FFM chooses the one corresponding to the field of  $j$ , i.e.,  $v_{i,F(j)}$ , where  $F(j)$  denotes the field of feature  $j$ .

Even though FFM has been proven more effective than FM, it's not widely deployed in industry due to its huge space complexity since it introduces  $M - 2$  times more parameters than FM, where  $M$  is usually at the magnitude of hundreds in practice. We tackle the high complexity of FFM by decoupling the number of embeddings per feature from the number of fields. Specifically, we group fields to  $P$  field parts and learn  $P$  embeddings for each feature, one for each field part. We choose a small  $P$  so as to reduce the total model size. Furthermore, we want to capture the field-pair-wise correlation to improve performance [42]. A straightforward implementation is to assign a weight for each field pair, but it leads to a computation cost of  $O(M^2)$ , which is unacceptable. To reduce the computation cost, we group fields into *field groups* and learn a weight for each field group pair.

$$\Phi = \sum_{i=1}^{\oplus} \sum_{j=i+1} x_i x_j \langle v_{i,P(j)}, v_{j,P(i)} \rangle r_{G(i),G(j)}, \quad (4)$$

where  $\oplus$  denotes element-wise summation,  $P(i)$  and  $G(i)$  denotes the field part or group of feature  $i$ , and  $r_{G(i),G(j)}$  denotes the learnable weights for field group pair  $(G(i), G(j))$ .

**Deployment Details.** In practice, we split all fields into two parts: the first one consists of all fields that are unrelated to the target ads, including all user and context side fields, while the second part includes all fields regarding the target ad. We then further split all fields of the first part into  $G$  groups based on expert knowledge, where  $G$  is at the dozens level, usually less than 50. We don't further split fields in the second part, that is, all fields in the second part belong to one field group. The GwPFM has been being deployed in our production since 2018, and still serves many modules and scenarios till now, mostly as the core expert.

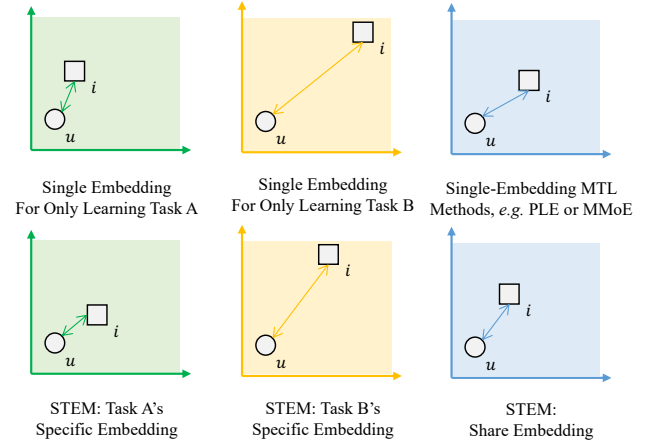


Figure 3: Illustration of interest entanglement in single-embedding based MTL models and disentanglement in STEM. The distance between embeddings of the user  $u$  and item  $i$  indicates the preference.

### 4.4 Beyond Multi-Embedding Paradigm: Collapse Resilient Feature Interaction

In addition to exploring multiple embeddings, we have conducted further investigation into the interaction function between two feature embeddings. The conventional approach, as employed in FM, conducts an element-wise inner product between the two embeddings:  $f(e_i, e_j) = e_i \odot e_j$ . However, recent research [27] has revealed that directly calculating the distance between two embeddings can lead to dimensional collapse. To address this issue, researchers verify that adding a projection matrix upon embeddings before computing the inner product can effectively mitigate the collapse [27]. We confirm its efficacy in ad recommendation, that is, incorporating a field-wise projection matrix  $W_{F(i) \rightarrow F(j)}$  within feature interaction [21, 51, 59] as done in DCN V2 can also mitigate the dimensional collapse of embeddings in recommendation. Specifically, the interaction function is defined as  $f(e_i, e_j) = (e_i W_{F(i) \rightarrow F(j)}) \odot e_j$ .

**Deployment Details.** Since 2021, DCN V2 is widely used as experts under the Heterogeneous Experts with Multi-Embedding framework mentioned before.

## 5 TACKLING INTEREST ENTANGLEMENT

User responses in ad recommender systems are driven by their complex interests under a specific task or scenario. Recently, there is a trend to train multiple tasks or scenarios together so as to leverage the information from more tasks/scenarios to enhance prediction accuracy. However, existing work mainly employ a shared-embedding paradigm, learning one embedding representation for each user and ad. This leads to a risk of entangling the learned embedding by the possibly contradictory user interests from various tasks or scenarios, resulting in negative transfer. Please refer to Fig. 3 for an illustration, where user's interest on an item is represented by the distance between their embeddings. In this section, we present two approaches to tackle interest entanglement for multi-task/scenario learning and auxiliary learning. In the following discussion, we take

multi-task learning as an example, and the same principle applies to multi-scenario learning, too.

## 5.1 AME for Multi-Task Learning

To tackle such an interest entanglement issue, we adopt a Shared and Task-specific EMbedding (STEM) paradigm [49], which *incorporates task-specific embeddings* to learn user's different interest across tasks, along with a shared embedding. The task-specific embeddings disentangle user and item representation (embeddings) across tasks, making it possible to preserve the distinct user interest in different tasks, as shown in Figure 3. We then employ a set of experts, where each expert is either task-specific, utilizing embeddings specific to a particular task, or shared across tasks, utilizing only shared embeddings.

However, there are a huge number of tasks in real-world ad recommendation systems. For example, each conversion type is usually treated as a task [41] when predicting conversions. There are usually dozens of conversion types, making learning an embedding table for each task infeasible. Therefore, in practice, we decouple the number of embedding tables from the number of tasks and rely on the gating mechanism to route between embedding tables to task towers. However, simply learning multiple embedding tables doesn't bring much performance gain as these embedding tables are symmetric to a large extent, and therefore can't be disentangled from each other.

To this end, we set different embedding sizes for these embedding tables to disentangle them, achieving an Asymmetric Multi-Embedding paradigm, or AME in short, as shown in Figure 4. Consequently, small tasks with fewer data need less model capacity and are routed via the gating more to the embedding tables with small sizes. In contrast, the other tasks with more data require larger model capacity and are routed to the large-size embedding tables.

*Connections to the Multi-Embedding Paradigm.* Multi-Embedding (ME) paradigm is mainly used for single-task learning to tackle the embedding dimensional collapse, while Shared and Task-Specific Embedding (STEM) and Asymmetric Multi-Embedding (AME) are mainly used to disentangle user interest representations across various tasks or scenarios. We try to use AME for single-task learning (e.g., click prediction) but brings little additional performance gain upon ME. Similarly, using ME for multi-task learning leads to Multi-Embedding MMoE (ME-MMoE) [49], which has been proven less effective than STEM [49] and AME (in our online test) since its embeddings are symmetric and hence may still be entangled.

*Deployment Details.* In practice, our conversion prediction model learns more than 100 conversion types simultaneously. We group these conversion types into 32 towers and adopt the asymmetric multi-embedding (AME) paradigm with three embedding tables of embedding sizes 16, 32, and 64, respectively. Compared to the single embedding baseline PLE, AME brings 0.32%, 0.24%, and 0.48% average AUC lifts for three representative scenarios (Moments, Official Accounts, and News), leading to 4.2%, 3.9%, and 7.1% GMV lift in our online A/B test. In particular, the AUC lifts in small tasks such as Pay are 0.35%, 0.27%, and 0.78% respectively, which are much larger than that on other large tasks.

## 5.2 STEM-AL for Auxiliary Learning

In industrial recommenders, sometimes we pay more attention to a main task and want to leverage the signals from other tasks to improve performance of the main task. For example, in click prediction, the main task is to predict the *convertible click*, which leads to the landing page for further conversions. Besides this valuable feedback, we also collect users' other behaviors regarding the ad: like, favorite, comment, dislike, and dwell time (on video ads). We'd like to resort to Auxiliary Learning (AL), using these additional auxiliary tasks to enhance the prediction of the convertible click.

To prevent these auxiliary tasks from entangling user's interest on the main task, we follow the STEM paradigm [49] and adopt a STEM-based Auxiliary Learning architecture, namely, STEM-AL. As shown in Figure 4, different from STEM and AME which pay equal attention to all tasks, STEM-AL treats one task (A) as the primary one and treats another Task (B) as an auxiliary task to improve the performance of A. In particular, STEM-AL makes the tower of the auxiliary task (B) only receive the forward from its corresponding expert. On the contrary, the tower of the main task (A) receives the forward from all tasks. In this way, the main task can benefit from the knowledge of all tasks, while the embeddings of the main task avoid being violated from other tasks, leading to the interest disentanglement between the main and auxiliary tasks. During inference, the auxiliary tower will be removed.

*Deployment Details.* We deploy STEM-AL to improve the pCTR in one scenario by samples from other domains. For example, we take the Applet pCTR as the main task and treat Moments pCTR as the auxiliary task. By using STEM-AL, the CTR of the main task can be improved by 1.16%. Further, if we use both Moments and Channel pCTR as the auxiliary task, the CTR on Applet can be improved by 2.93%.

## 6 MODEL TRAINING

Building upon our earlier discussions, it becomes evident that representation learning plays a pivotal role in laying the foundation for a robust recommendation system. In addition, we have crafted several sophisticated model training techniques to complement representation learning, thereby enhancing the overall expressive capabilities of our recommendation system. Commonly, the CTR prediction task is tackled naively in a pure supervised learning which can be denoted as:  $\mathcal{L} = 1/N \sum_{i=1}^N \text{BCE}(y_i, f(x_i))$ , here  $\{y_1, y_2, \dots, y_N\}$  denotes labels which  $y_i = 1$  denotes click and  $y_i = 0$  denotes non-click,  $\{x_1, x_2, \dots, x_N\}$  corresponds to input, and  $\text{BCE}(y_i, f_i) = -y_i \log \sigma(f_i) - (1 - y_i) \log(1 - \sigma(f_i))$  corresponds to the Binary Cross Entropy (BCE). We figure out certain issues within the naive supervised learning structure which will be detailed in the following subsections.

### 6.1 Gradient Vanishing and Ranking Loss

Recent work [32, 46] finds out that incorporating ranking loss with BCE loss has shown substantial performance improvement in online advertising. However, the efficacy of this combination form is not fully comprehended. Our recent research [35] examines its efficiency from a new perspective: that negative samples suffer from *gradient vanishing* with only BCE loss when the positive feedback



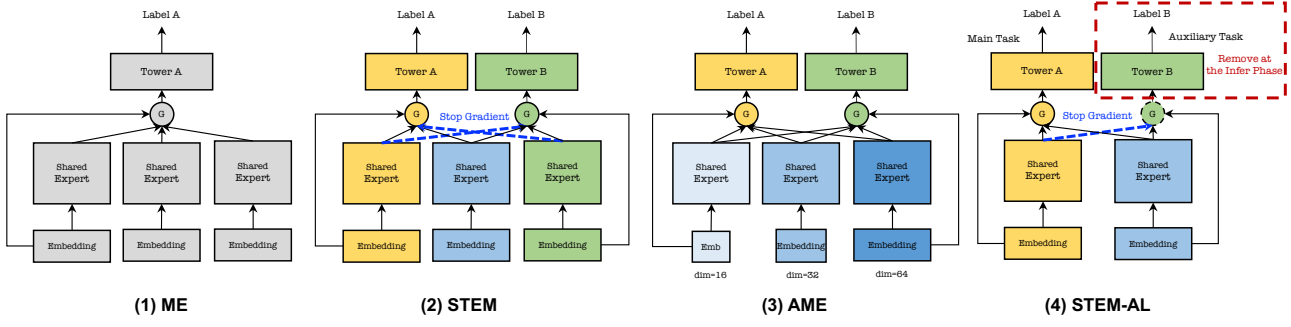


**Figure 4: Comparison among various paradigms: Multi-Embedding (ME), Shared and Task-Specific Embedding (STEM), Asymmetric Multi-Embedding (AME), and STEM for Auxiliary Learning (STEM-AL).** ME aims to optimize a single task, and learns multiple embeddings to tackle dimensional collapse. STEM and AME is used for multi-task learning, where STEM learns task-specific embeddings, and AME learns task-decoupled yet disentangled embeddings with different size. STEM-AL is for auxiliary learning, learns a task-specific embedding for the main task, and an additional embedding updated by multiple tasks.

are sparse, such as in our pCTR model, where 0.1% to 1% samples are positive (click). Instead, after combining BCE with the ranking loss, we show empirically and theoretically that the gradients become significantly larger [35]. This leads to a lower BCE loss on both test samples (indicating better classification ability) and training samples (indicating easier optimization). We kindly advice readers refer to [35] for more details.

**Deployment Details.** The combination of ranking loss with BCE loss is widely deployed in the Moments and Channel pCTR models, with GMV lift of 0.57% and 1.08%, respectively. It's also deployed in all pLTV models, with a LTV GMV lift of 5.99%. Besides, the prediction bias is also improved, especially on samples with low prediction score.

## 6.2 Repeated Exposure and Weighted Sampling

Repetitive exposure, that is, displaying the same or similar ads to users within a short period, can enhance user's perception on specific ads, but may also risk harming user experience. To tackle this, we introduced the *Repetitive Exposure Weight* (REW) module to decrease the prediction score of repeated ads for a given user, so as to reduce their exposure. The core idea is to assign a higher weights for the repeated impression (negative sample) of ads.

Specifically, for each repeated impression, we assign a weight  $w_{rep} \geq 1$  to the original loss:  $\mathcal{L} = \frac{1}{N} \sum_{i=1}^N w_{rep} \cdot \text{BCE}(y_i, f(x_i))$ . It considers both the repeated count as well as recency:  $w_{rep} = \alpha \cdot w_{count} + (1 - \alpha) \cdot w_{recency}$ , where  $w_{count}$  equals to the total number of exposure (time decayed) of the same or similar ad to this user, and  $w_{recency}$  denotes the time gap in days between the last repeated impression and the current time. Please note that these weight would lead bias to the whole model since it downweights negative samples of repeated exposure. We rectify such bias by involving a weight  $w_{debias} = (\sum_{i=1}^N (1 - y_i) \cdot w_{rep} / \sum_{i=1}^N (1 - y_i))$  for all positive samples.

**Deployment Details.** The REW module is widely deployed in Tencent Official Accounts, News, and Video pCTR models, reducing percentage of repetitive exposure ads by 14.7%, 7.8%, and 9.7% respectively.

## 6.3 Online Learning

We train both our pCTR and pCVR models with online learning, where samples are populated to the models in seconds. Online learning for pCVR poses special challenge due to conversion delay feedback. There is a lot of work [8, 65] to address it. Nevertheless, these method will lead to pronounced model bias due to substantial fluctuations of conversion feedback in Tencent ad system. For instance, certain advertisers may report all previous conversions at uncertain times, resulting in an exceptionally high observed CVR at that moment, while reporting 0 at other times. In response to these challenges, we propose a dynamic online learning method based on the conversion feedback variance. Specifically, a very small variance means that the observed CVR is close to the history CVR, so we can populate the samples as fast as possible. Otherwise when the variance is large, we will set a waiting time to ensure the stability of conversion arrival and hence reduce the risk of high bias due to arrival fluctuation.

**Deployment Details.** Our approach has been implemented in various scenerios for Tencent Ads, including pCVR models for Tencent Moments, Channel and Official accounts, with overall GMV lift of 0.3%, 1.49%, 1.14%, and new ad GMV lift of 2.48%, 0.8%, 4.34% respectively, where the new ad refers to ad that has been online within 3 days. Besides, bias of new ads in all scenarios has decreased from over 10% to within 1%.

## 6.4 Exploration with Uncertainty Estimates

So far our focus primarily lies in enhancing the models' ability to accurately predict click or conversion rates, utilizing these scores to rank ads and maximize exploitation, while neglecting the importance of exploration. However, extensive research has demonstrated the criticality of striking a balance between exploration and exploitation, particularly for cold-start ads. Consequently, we propose adopting a Bayesian perspective for CTR modeling, wherein instead of predicting a single point estimate for CTR, we predict a distribution that incorporates uncertainty estimations.

To achieve this, we introduce a Gaussian process (GP) prior distribution to represent the unknown true CTR function. By leveraging

observed data, we obtain predictions and uncertainty estimations from the posterior distribution. Combining these uncertainty estimates with well-established bandit algorithms, specifically Thompson Sampling (TS), enables us to effectively manage the exploration-exploitation trade-off and enhance long-term utilities.

$$\text{pCTR}_{\text{TS}} = \sigma(\hat{f}) \text{ where } \hat{f} \sim \mathcal{N}(\mu(\mathbf{x}^*), \Sigma(\mathbf{x}^*)) \quad (5)$$

where  $\mu(\mathbf{x}^*)$  and  $\Sigma(\mathbf{x}^*)$  denotes the mean and variance of the posterior logit value  $f(\mathbf{x}^*)$  for test data point  $\mathbf{x}^*$ .

*Deployment Details.* The GP-based model is deployed in Tencent Moments pCTR, with GMV lift of +1.92%.

## 7 ANALYSIS TOOLS

In this section, we present several off-the-shelf analysis tools on representation learning to: analyze the correlation between features, check whether and to what extent embeddings collapse, and the entanglement of user interest. These tools are key to unveiling neglected issues of existing methods, motivating us to propose novel approaches to tackle these issues.

### 7.1 Feature Correlation

We can measure both *ground-truth* and *learned* feature correlation on particular samples or feature combinations via mutual information [42, 72]. The ground-truth correlation can be calculated by the mutual information between features  $X$  and the user's response (label)  $Y$  under certain constraints. In particular, when handling sequential features, we'd like to measure the semantic-temporal correlation between behaviors with specific categories whilst at specific position  $X_{\text{con}_b}$ , and the user's response on targets of specific categories  $Y_{\text{con}_t}$ . After defining the constraints on behaviors and the target, e.g.,  $\text{con}_b$  and  $\text{con}_t$ , the correlation can be quantified as

$$\text{Cor} = \text{MI}(X_{\text{con}_b}, Y_{\text{con}_t}) \quad (6)$$

For example, we can first select a subset of samples with target category  $c_t$ , and then for behaviors with category  $c_b$  whilst at various positions  $p$  (or with various time intervals), we can quantify the correlation as

$$\text{Cor} = \text{MI}(X_{C(X)=c_b \wedge P(X)=p}, Y_{C(Y)=c_t}) \quad (7)$$

We can also quantify the learned correlation of a specific model. Please kindly refer to [72] for details.

### 7.2 Embedding Dimensional Collapse

Dimensional collapse happens when embedding vectors span in a lower-dimensional subspace. Following [27], we can measure dimensional collapse by conduct a singular value decomposition (SVD) of the embedding matrix of each field. In particular, given an embedding matrix of field  $i$ :  $E_i \in \mathbb{R}^{N_i \times K}$ , after the SVD  $E_i = U\Sigma V^*$ ,  $\Sigma = \text{diag}(\sigma^k)$ , we can get the singular values  $\sigma_k$ . Dimensional collapse happens when some singular values are small. Besides, we can further define quantify the dimensional collapse of an embedding matrix by a new metric: Information Abundance (IA) [21], which is defined as the the sum of all singular values

normalized by the maximum singular value. The smaller the IA, the more embeddings collapse dimensionally.

### 7.3 Interest Entanglement

User response in ads recommender systems are driven by the complex interactions of many factors behind the users' decision making processes. We can measure such factor entanglement by first selecting a set of contradictory user-item pairs  $S$  whose embedding distance are large in one task but low in another one. We then plot the distance distribution of  $S$  based on: a) embeddings from two single task model, b) the embeddings of a shared-embedding based multi-task learning model, e.g., PLE, c) the embeddings of each task as well as the shared embedding in STEM. We do observe that PLE fail to capture entangled interest on this set, while STEM succeeds.

## 8 RELATED WORK

**Feature Encoding.** Modeling sequence of user behaviors have been widely studied [10, 16, 25, 29, 43, 50, 70, 71]. Regarding numerical features, existing work can be categorized into two groups: non-discretization [13, 40, 44] and discretization [9, 19]. Recently, with a huge growth research on LLM, lots work study how to utilize embeddings learned from these external pre-trained models in recommender systems [69].

**Feature Interactions and Dimensional Collapse.** There are numerous work on the backbone architecture with explicit or implicit feature interaction, from the shallow models FM [45], FFM [28], FwFM [42] and FmFM [51], to deep models such as Wide & Deep [12], DeepFM [20], xDeepFM [34], AutoInt [48], DCN V2 [59]. Refer to [64, 66] for a comprehensive survey.

The complete collapse has been widely studied in self-supervised learning (SSL) [11, 60], and Mixtures-of-Experts (MoE) [27]. On the other hand, dimensional collapse has been studied in SSL [26] and contrastive learning [27].

**Interest Entanglement under MTL and MDL.** Negative transfer has been a key challenge in Multi-Task Learning (MTL) and Multi-Domain Learning (MDL). Shared-embedding paradigm is widely adopted in either MTL [6, 37, 41, 52] and MDL [7, 47, 73]. Disentangled Representation Learning (DRL) aims to identify and disentangle the underlying explanatory factors [3] in embeddings, and has also been used in recommendation [62].

**Industrial Architecture.** There are already several work on industrial recommender systems [13, 14, 18, 24, 39, 58]. We differ from these work in the sense that we pay more attention to the representation, especially from a dimensional collapse and interest entanglement perspective.

## 9 CONCLUSION

In this paper, we describe an industry ad recommendation system, paying special attention to the representation learning perspective. We present how to encode features with inherent priors, as well as practices to tackle the dimensional collapse and interest entanglement issue. We also showcase several training tricks as well as analysis tools. We hope this work can shed light on the future development of this research area.



## REFERENCES

- [1] Josh Achiam, Steven Adler, Sandhini Agarwal, Lama Ahmad, Ilge Akkaya, Florencia Leoni Aleman, Diogo Almeida, Janko Altmenschmidt, Sam Altman, Shyamal Anadkat, et al. 2023. Gpt-4 technical report. *arXiv preprint arXiv:2303.08774* (2023).
- [2] Newsha Ardalani, Carole-Jean Wu, Zeliang Chen, Bhargav Bhushanam, and Adnan Aziz. 2022. Understanding Scaling Laws for Recommendation Models. *arXiv preprint arXiv:2208.08489* (2022).
- [3] Yoshua Bengio, Aaron Courville, and Pascal Vincent. 2013. Representation learning: A review and new perspectives. *IEEE transactions on pattern analysis and machine intelligence* 35, 8 (2013), 1798–1828.
- [4] Yoshua Bengio and Olivier Delalleau. 2011. On the expressive power of deep architectures. In *International conference on algorithmic learning theory*. Springer, 18–36.
- [5] Yoshua Bengio, Olivier Delalleau, and Nicolas Roux. 2005. The curse of highly variable functions for local kernel machines. *Advances in neural information processing systems* 18 (2005).
- [6] Rich Caruana. 1997. Multitask learning. *Machine learning* 28, 1 (1997), 41–75.
- [7] Jianxin Chang, Chenbin Zhang, Yiqun Hui, Dewei Leng, Yanan Niu, Yang Song, and Kun Gai. 2023. Pepnet: Parameter and embedding personalized network for infusing with personalized prior information. In *Proceedings of the 29th ACM SIGKDD Conference on Knowledge Discovery and Data Mining*. 3795–3804.
- [8] Olivier Chapelle. 2014. Modeling delayed feedback in display advertising. In *Proceedings of the 20th ACM SIGKDD international conference on Knowledge discovery and data mining*. 1097–1105.
- [9] Bo Chen, Huifeng Guo, Weiwen Liu, Yue Ding, Yunzhe Li, Wei Guo, Yichao Wang, Zhicheng He, Ruiming Tang, and Rui Zhang. 2022. Numerical Feature Representation with Hybrid N-ary Encoding. In *Proceedings of the 31st ACM International Conference on Information & Knowledge Management*. 2984–2993.
- [10] Qiwei Chen, Huan Zhao, Wei Li, Pipei Huang, and Wenwu Ou. 2019. Behavior sequence transformer for e-commerce recommendation in alibaba. In *Proceedings of the 1st International Workshop on Deep Learning Practice for High-Dimensional Sparse Data*. 1–4.
- [11] Ting Chen, Simon Kornblith, Mohammad Norouzi, and Geoffrey Hinton. 2020. A simple framework for contrastive learning of visual representations. In *International conference on machine learning*. PMLR, 1597–1607.
- [12] Heng-Tze Cheng, Levent Koc, Jeremiah Harmsen, Tal Shaked, Tushar Chandra, Hrishii Aradhye, Glen Anderson, Greg Corrado, Wei Chai, Mustafa Ipsir, et al. 2016. Wide & deep learning for recommender systems. In *Proceedings of the 1st workshop on deep learning for recommender systems*. 7–10.
- [13] Paul Covington, Jay Adams, and Emre Sargin. 2016. Deep neural networks for youtube recommendations. In *Proceedings of the 10th ACM conference on recommender systems*. 191–198.
- [14] James Davidson, Benjamin Liebald, Junning Liu, Palash Nandy, Taylor Van Vleet, Ullas Gargi, Sujoy Gupta, Yu He, Mike Lambert, Blake Livingston, et al. 2010. The YouTube video recommendation system. In *Proceedings of the fourth ACM conference on Recommender systems*. 293–296.
- [15] Jacob Devlin, Ming-Wei Chang, Kenton Lee, and Kristina Toutanova. 2018. Bert: Pre-training of deep bidirectional transformers for language understanding. *arXiv preprint arXiv:1810.04805* (2018).
- [16] Yufei Feng, Fuyu Lv, Weichen Shen, Menghan Wang, Fei Sun, Yu Zhu, and Keping Yang. 2019. Deep session interest network for click-through rate prediction. In *International Joint Conference on Artificial Intelligence (IJCAI)*. 2301–2307.
- [17] Tao Gong, Chengqi Lyu, Shilong Zhang, Yudong Wang, Miao Zheng, Qian Zhao, Kuikun Liu, Wenwei Zhang, Ping Luo, and Kai Chen. 2023. Multimodal-gpt: A vision and language model for dialogue with humans. *arXiv preprint arXiv:2305.04790* (2023).
- [18] Mihajlo Grbovic and Haibin Cheng. 2018. Real-time personalization using embeddings for search ranking at airbnb. In *Proceedings of the 24th ACM SIGKDD international conference on knowledge discovery & data mining*. 311–320.
- [19] Huifeng Guo, Bo Chen, Ruiming Tang, Weinan Zhang, Zhenguo Li, and Xiuqiang He. 2021. An embedding learning framework for numerical features in ctr prediction. In *Proceedings of the 27th ACM SIGKDD Conference on Knowledge Discovery & Data Mining*. 2910–2918.
- [20] Huifeng Guo, Ruiming Tang, Yunming Ye, Zhenguo Li, and Xiuqiang He. 2017. DeepFM: a factorization-machine based neural network for CTR prediction. *arXiv preprint arXiv:1703.04247* (2017).
- [21] Xingzhuo Guo, Junwei Pan, Ximei Wang, Baixu Chen, Jie Jiang, and Mingsheng Long. 2023. On the Embedding Collapse when Scaling up Recommendation Models. *arXiv preprint arXiv:2310.04400* (2023).
- [22] Will Hamilton, Zitao Ying, and Jure Leskovec. 2017. Inductive representation learning on large graphs. *Advances in neural information processing systems* 30 (2017).
- [23] Kaiming He, Xiangyu Zhang, Shaoqing Ren, and Jian Sun. 2016. Deep residual learning for image recognition. In *Proceedings of the IEEE conference on computer vision and pattern recognition*. 770–778.
- [24] Xinran He, Junfeng Pan, Ou Jin, Tianbing Xu, Bo Liu, Tao Xu, Yanxin Shi, Antoine Atallah, Ralf Herbrich, Stuart Bowers, et al. 2014. Practical lessons from predicting clicks on ads at facebook. In *International Workshop on Data Mining for Online Advertising (ADKDD)*. 1–9.
- [25] Balázs Hidasi, Alexandros Karatzoglou, Linas Baltrunas, and Domonkos Tikk. 2015. Session-based recommendations with recurrent neural networks. *arXiv preprint arXiv:1511.06939* (2015).
- [26] Tianyu Hua, Wenxiao Wang, Zihui Xue, Sucheng Ren, Yue Wang, and Hang Zhao. 2021. On feature decorrelation in self-supervised learning. In *Proceedings of the IEEE/CVF International Conference on Computer Vision*. 9598–9608.
- [27] Li Jing, Pascal Vincent, Yann LeCun, and Yuandong Tian. 2021. Understanding Dimensional Collapse in Contrastive Self-supervised Learning. In *ICLR*.
- [28] Yuchin Juan, Yong Zhuang, Wei-Sheng Chin, and Chih-Jen Lin. 2016. Field-aware factorization machines for CTR prediction. In *Proceedings of the 10th ACM Conference on Recommender Systems (RecSys)*. 43–50.
- [29] Wang-Cheng Kang and Julian McAuley. 2018. Self-attentive sequential recommendation. In *2018 IEEE International Conference on Data Mining (ICDM)*. IEEE, 197–206.
- [30] Yehuda Koren, Robert Bell, and Chris Volinsky. 2009. Matrix factorization techniques for recommender systems. *Computer* 42, 8 (2009), 30–37.
- [31] Alex Krizhevsky, Ilya Sutskever, and Geoffrey E Hinton. 2012. Imagenet classification with deep convolutional neural networks. In *NeurIPS*.
- [32] Cheng Li, Yue Lu, Qiaozhu Mei, Dong Wang, and Sandeep Pandey. 2015. Click-through prediction for advertising in twitter timeline. In *Proceedings of the 21th ACM SIGKDD International Conference on Knowledge Discovery and Data Mining*. 1959–1968.
- [33] Xiangyang Li, Bo Chen, Lu Hou, and Ruiming Tang. 2023. CTRL: Connect Tabular and Language Model for CTR Prediction. *arXiv preprint arXiv:2306.02841* (2023).
- [34] Jianxun Lian, Xiaohuan Zhou, Fuzheng Zhang, Zhongxia Chen, Xing Xie, and Guangzhong Sun. 2018. xdeepfm: Combining explicit and implicit feature interactions for recommender systems. In *Proceedings of the 24th ACM SIGKDD International Conference on Knowledge Discovery and Data Mining (SIGKDD)*. 1754–1763.
- [35] Zhutian Lin, Juwei Pan, Shangyu Zhang, Ximei Wang, Xi Xiao, Shudong Huang, Lei Xiao, and Jie Jiang. 2024. Understanding the Ranking Loss for Recommendation with Sparse User Feedback. *arXiv preprint* (2024).
- [36] Fan Liu, Huilin Chen, Zhiyong Cheng, Anan Liu, Liqiang Nie, and Mohan Kankanhalli. 2022. Disentangled multimodal representation learning for recommendation. *IEEE Transactions on Multimedia* (2022).
- [37] Jiaqi Ma, Zhe Zhao, Xinyang Yi, Jilin Chen, Lichan Hong, and Ed H. Chi. 2018. Modeling Task Relationships in Multi-task Learning with Multi-gate Mixture-of-Experts. In *KDD*. ACM, 1930–1939.
- [38] Kelong Mao, Jieming Zhu, Liangcai Su, Guohao Cai, Yuru Li, and Zhenhua Dong. 2023. FinalMLP: An Enhanced Two-Stream MLP Model for CTR Prediction. *arXiv preprint arXiv:2304.00902* (2023).
- [39] H Brendan McMahan, Gary Holt, David Sculley, Michael Young, Dietmar Ebner, Julian Grady, Lan Nie, Todd Phillips, Eugene Davydov, Daniel Golovin, et al. 2013. Ad click prediction: a view from the trenches. In *ACM SIGKDD International conference on Knowledge Discovery & Data Mining (KDD)*. 1222–1230.
- [40] Maxim Naumov, Dheevatsa Mudigere, Hao-Jun Michael Shi, Jianyu Huang, Narayanan Sundaraman, Jongsoo Park, Xiaodong Wang, Udit Gupta, Carole-Jean Wu, Alisson G Azzolini, et al. 2019. Deep learning recommendation model for personalization and recommendation systems. *arXiv preprint arXiv:1906.00091* (2019).
- [41] Junwei Pan, Yizhi Mao, Alfonso Lobos Ruiz, Yu Sun, and Aaron Flores. 2019. Predicting different types of conversions with multi-task learning in online advertising. In *Proceedings of the 25th ACM SIGKDD International Conference on Knowledge Discovery & Data Mining*. 2689–2697.
- [42] Junwei Pan, Jian Xu, Alfonso Lobos Ruiz, Wenliang Zhao, Shengjun Pan, Yu Sun, and Quan Lu. 2018. Field-weighted factorization machines for click-through rate prediction in display advertising. In *Proceedings of the 2018 World Wide Web Conference (WWW)*. 1349–1357.
- [43] Qi Pi, Guorui Zhou, Yujing Zhang, Zhe Wang, Lejian Ren, Ying Fan, Xiaoqiang Zhu, and Kun Gai. 2020. Search-based user interest modeling with lifelong sequential behavior data for click-through rate prediction. In *ACM International Conference on Information & Knowledge Management (CIKM)*. 2685–2692.
- [44] Yanru Qu, Han Cai, Kan Ren, Weinan Zhang, Yong Yu, Ying Wen, and Jun Wang. 2016. Product-based neural networks for user response prediction. In *2016 IEEE 16th International Conference on Data Mining (ICDM)*. IEEE, 1149–1154.
- [45] Steffen Rendle. 2010. Factorization machines. In *2010 IEEE International Conference on Data Mining (ICDM)*. IEEE, 995–1000.
- [46] Xiang-Rong Sheng, Jingyue Gao, Yueyao Cheng, Siran Yang, Shuguang Han, Hongbo Deng, Yuning Jiang, Jian Xu, and Bo Zheng. 2023. Joint Optimization of Ranking and Calibration with Contextualized Hybrid Model. In *Proceedings of the 29th ACM SIGKDD Conference on Knowledge Discovery and Data Mining*. 4813–4822.
- [47] Xiang-Rong Sheng, Liqin Zhao, Guorui Zhou, Xinyao Ding, Binding Dai, Qiang Luo, Siran Yang, Jingshan Lv, Chi Zhang, Hongbo Deng, et al. 2021. One model to

- serve all: Star topology adaptive recommender for multi-domain ctr prediction. In *Proceedings of the 30th ACM International Conference on Information & Knowledge Management*. 4104–4113.
- [48] Weiping Song, Chence Shi, Zhiping Xiao, Zhijian Duan, Yewen Xu, Ming Zhang, and Jian Tang. 2019. Autoint: Automatic feature interaction learning via self-attentive neural networks. In *Proceedings of the 28th ACM International Conference on Information and Knowledge Management (CIKM)*. 1161–1170.
- [49] Liangcai Su, Junwei Pan, Ximei Wang, Xi Xiao, Shijie Quan, Xihua Chen, and Jie Jiang. 2023. STEM: Unleashing the Power of Embeddings for Multi-task Recommendation. *arXiv preprint arXiv:2308.13537* (2023).
- [50] Fei Sun, Jun Liu, Jian Wu, Changhua Pei, Xiao Lin, Wenwu Ou, and Peng Jiang. 2019. BERT4Rec: Sequential recommendation with bidirectional encoder representations from transformer. In *ACM International Conference on Information and Knowledge Management (CIKM)*. 1441–1450.
- [51] Yang Sun, Junwei Pan, Alex Zhang, and Aaron Flores. 2021. Fm2: Field-matrixed factorization machines for recommender systems. In *Proceedings of the Web Conference 2021*. 2828–2837.
- [52] Hongyan Tang, Junning Liu, Ming Zhao, and Xudong Gong. 2020. Progressive Layered Extraction (PLE): A Novel Multi-Task Learning (MTL) Model for Personalized Recommendations. In *RecSys*. ACM, 269–278.
- [53] Zhen Tian, Ting Bai, Wayne Xin Zhao, Ji-Rong Wen, and Zhao Cao. 2023. EulerNet: Adaptive Feature Interaction Learning via Euler’s Formula for CTR Prediction. *arXiv preprint arXiv:2304.10711* (2023).
- [54] Hugo Touvron, Thibaut Lavril, Gautier Izacard, Xavier Martinet, Marie-Anne Lachaux, Timothée Lacroix, Baptiste Rozière, Naman Goyal, Eric Hambro, Faisal Azhar, et al. 2023. Llama: Open and efficient foundation language models. *arXiv preprint arXiv:2302.13971* (2023).
- [55] Ashish Vaswani, Noam Shazeer, Niki Parmar, Jakob Uszkoreit, Llion Jones, Aidan N Gomez, Łukasz Kaiser, and Illia Polosukhin. 2017. Attention is all you need. In *NeurIPS*.
- [56] Fangye Wang, Yingxu Wang, Dongsheng Li, Hansu Gu, Tun Lu, Peng Zhang, and Ning Gu. 2023. CL4CTR: A Contrastive Learning Framework for CTR Prediction. In *Proceedings of the Sixteenth ACM International Conference on Web Search and Data Mining*. 805–813.
- [57] Hongya Wang, Jiao Cao, LihChyun Shu, and Davood Rafiei. 2013. Locality sensitive hashing revisited: filling the gap between theory and algorithm analysis. In *Proceedings of the 22nd ACM International Conference on Information & Knowledge Management (San Francisco, California, USA) (CIKM '13)*. Association for Computing Machinery, New York, NY, USA, 1969–1978. <https://doi.org/10.1145/2505515.2505765>
- [58] Jun Wang, Weinan Zhang, Shuai Yuan, et al. 2017. Display advertising with real-time bidding (RTB) and behavioural targeting. *Foundations and Trends® in Information Retrieval* 11, 4-5 (2017), 297–435.
- [59] Ruoxi Wang, Rakesh Shivanna, Derek Cheng, Sagar Jain, Dong Lin, Lichan Hong, and Ed Chi. 2021. DCN-V2: Improved deep & cross network and practical lessons for web-scale learning to rank systems. In *Proceedings of the Web Conference (WWW)*. 1785–1797.
- [60] Tongzhou Wang and Phillip Isola. 2020. Understanding contrastive representation learning through alignment and uniformity on the hypersphere. In *International Conference on Machine Learning*. PMLR, 9929–9939.
- [61] Xin Wang, Hong Chen, Si’ao Tang, Zihao Wu, and Wenwu Zhu. 2022. Disentangled representation learning. *arXiv preprint arXiv:2211.11695* (2022).
- [62] Xin Wang, Hong Chen, Yuwei Zhou, Jianxin Ma, and Wenwu Zhu. 2022. Disentangled representation learning for recommendation. *IEEE Transactions on Pattern Analysis and Machine Intelligence* 45, 1 (2022), 408–424.
- [63] Christopher KI Williams and Carl Edward Rasmussen. 2006. *Gaussian processes for machine learning*. Vol. 2. MIT press Cambridge, MA.
- [64] Yanwu Yang and Panyu Zhai. 2022. Click-through rate prediction in online advertising: A literature review. *Information Processing & Management* 59, 2 (2022), 102853.
- [65] Shota Yasui, Gota Morishita, Fujita Komei, and Masashi Shibata. 2020. A feedback shift correction in predicting conversion rates under delayed feedback. In *Proceedings of The Web Conference 2020*. 2740–2746.
- [66] Shuai Zhang, Lina Yao, Aixin Sun, and Yi Tay. 2019. Deep learning based recommender system: A survey and new perspectives. *ACM computing surveys (CSUR)* 52, 1 (2019), 1–38.
- [67] Weinan Zhang, Jiarui Qin, Wei Guo, Ruiming Tang, and Xiuqiang He. 2021. Deep learning for click-through rate estimation. *arXiv preprint arXiv:2104.10584* (2021).
- [68] Wayne Xin Zhao, Kun Zhou, Junyi Li, Tianyi Tang, Xiaolei Wang, Yupeng Hou, Yingqian Min, Beichen Zhang, Junjie Zhang, Zican Dong, et al. 2023. A survey of large language models. *arXiv preprint arXiv:2303.18223* (2023).
- [69] Bowen Zheng, Yupeng Hou, Hongyu Lu, Yu Chen, Wayne Xin Zhao, and Ji-Rong Wen. 2023. Adapting large language models by integrating collaborative semantics for recommendation. *arXiv preprint arXiv:2311.09049* (2023).
- [70] Guorui Zhou, Na Mou, Ying Fan, Qi Pi, Weijie Bian, Chang Zhou, Xiaoqiang Zhu, and Kun Gai. 2019. Deep interest evolution network for click-through rate prediction. In *AAAI Conference on Artificial Intelligence (AAAI)*. Vol. 33. 5941–5948.
- [71] Guorui Zhou, Xiaoqiang Zhu, Chenru Song, Ying Fan, Han Zhu, Xiao Ma, Yanghui Yan, Junqi Jin, Han Li, and Kun Gai. 2018. Deep interest network for click-through rate prediction. In *ACM SIGKDD International Conference on Knowledge Discovery & Data Mining (KDD)*. 1059–1068.
- [72] Haolin Zhou, Junwei Pan, Xinyi Zhou, Xihua Chen, Jie Jiang, Xiaofeng Gao, and Guihai Chen. 2023. Temporal Interest Network for Click-Through Rate Prediction. *arXiv preprint arXiv:2308.08487* (2023).
- [73] Jie Zhou, Xianshuai Cao, Wenhao Li, Kun Zhang, Chuan Luo, and Qian Yu. 2023. HiNet: A Novel Multi-Scenario & Multi-Task Learning Approach with Hierarchical Information Extraction. *arXiv preprint arXiv:2303.06095* (2023).
- [74] Kun Zhou, Hui Wang, Wayne Xin Zhao, Yutao Zhu, Sirui Wang, Fuzheng Zhang, Zhongyuan Wang, and Ji-Rong Wen. 2020. S3-rec: Self-supervised learning for sequential recommendation with mutual information maximization. In *Proceedings of the 29th ACM international conference on information & knowledge management*. 1893–1902.

## A APPENDIX

### A.1 Exploration with Uncertainty Estimates

**A.1.1 Gaussian Process for CTR prediction.** A GP prior distribution assumption over  $f \sim \mathcal{GP}(m_\theta(\mathbf{x}), k_\theta(\mathbf{x}, \mathbf{x}'))$  where  $m(\mathbf{x}) = \mathbb{E}[f(\mathbf{x})]$  denotes the mean function and  $k_\theta(\mathbf{x}, \mathbf{x}') = \mathbb{E}[(f(\mathbf{x}) - m(\mathbf{x}))(f(\mathbf{x}') - m(\mathbf{x}'))]$  denotes the covariance function in which  $\mathbf{x}$  and  $\mathbf{x}'$  denote different input locations where the function  $f$  is evaluated, and  $\theta$  denotes the set of hyperparameters of the kernel functions. A common choice for the mean function is  $m(\mathbf{x}) = 0$  (since the prior knowledge and uncertainty about the mean function can be taken into account by adjusting the kernel function).

After accounting for the mean function, the GP is fully specified by the form of the covariance/kernel function and the associated hyperparameters  $\theta$ .

The task typically involves predicting the latent function value  $f^\star = f(\mathbf{x}^\star)$  at an unseen test input  $\mathbf{x}^\star$ . Let  $\mathbf{X} \triangleq \{\mathbf{x}_n\}_{n=1}^N$  denotes the training data inputs,  $\mathbf{f} \triangleq \{f(\mathbf{x}_n)\}_{n=1}^N$  represents the latent function values, and  $\mathbf{y} \triangleq \{y_n\}_{n=1}^N$  be the user feedback (click or not). Here each feedback  $y_n$  is corrupted as a noisy measurement of latent function values  $f(\mathbf{x}_n)$  by a Bernoulli likelihood  $p(y_n|f(\mathbf{x}_n)) = \text{Ber}(y_n; \sigma(f(\mathbf{x}_n)))$  where  $\sigma(\cdot)$  corresponds to the sigmoid function. Then the joint distribution of  $\{f^\star, \mathbf{f}, \mathbf{y}\}$  can be written as  $p(f^\star, \mathbf{f}, \mathbf{y}) = p(f^\star, \mathbf{f})p(\mathbf{y}|\mathbf{f})$  and  $p(\mathbf{y}|\mathbf{f}) = \prod_{n=1}^N \text{Ber}(y_n; \sigma(f(\mathbf{x}_n)))$ .

The joint distribution  $p(f^\star, \mathbf{f})$  can be represented with a multivariate normal distribution:

$$\begin{bmatrix} f^\star \\ \mathbf{f} \end{bmatrix} \sim \mathcal{N}\left(\begin{bmatrix} 0 \\ 0 \end{bmatrix}, \begin{bmatrix} k_{\mathbf{x}^\star \mathbf{x}^\star} & \mathbf{k}_{\mathbf{x}^\star \mathbf{X}} \\ \mathbf{k}_{\mathbf{X} \mathbf{x}^\star} & \mathbf{K}_{\mathbf{X} \mathbf{X}} \end{bmatrix}\right) \quad (8)$$

where  $k_{\mathbf{x}^\star \mathbf{x}^\star} = k_\theta(\mathbf{x}^\star, \mathbf{x}^\star)$  is the variance of the test function value,  $\mathbf{k}_{\mathbf{x}^\star \mathbf{X}} \triangleq \mathbf{k}_{\mathbf{X} \mathbf{x}^\star}^\top$  and  $\mathbf{k}_{\mathbf{x}^\star \mathbf{X}}$  denotes a vector with components  $k_\theta(\mathbf{x}^\star, \mathbf{x}_n)$  for  $n = 1, 2, \dots, N$ .  $\mathbf{K}_{\mathbf{X} \mathbf{X}}$  denotes the covariance matrix with components  $k_\theta(\mathbf{x}_n, \mathbf{x}_{n'})$  for  $n, n' = 1, 2, \dots, N$ .

Therefore, the posterior distribution of  $f^\star$  given observations  $\mathbf{y}$  can be rewritten as:  $p(f^\star|\mathbf{y}) = 1/p(\mathbf{y}) \int p(\mathbf{y}|\mathbf{f})p(f^\star, \mathbf{f})d\mathbf{f}$ .

This suggests that the predictive distribution of the function value at an unseen test input is Gaussian-distributed with the posterior mean and variance. In this regard, a GP can be seen as a prior

over the function  $f$ . Conditioning this prior on the training data results in a posterior that 'fits' the data. Please refer to Williams and Rasmussen [63] for more details.

### A.2 Feature Correlation

We present such semantic-temporal correlation in our production dataset in Fig. 5. In particular, we pickup a target category A, and calculate the ground-truth correlation of behaviors belong to various categories (A to J along y-axis) with different time intervals or at relative positions regarding the target. Among all history behaviors, those belong to the same category with target, *i.e.*, the 1st row in both figures, are more correlated to user's response on target. In addition, there is a strong time-decaying pattern among these behaviors of category A, that is, those close to the target temporally are more informative. Such decaying pattern is more strong on time intervals than relative position.

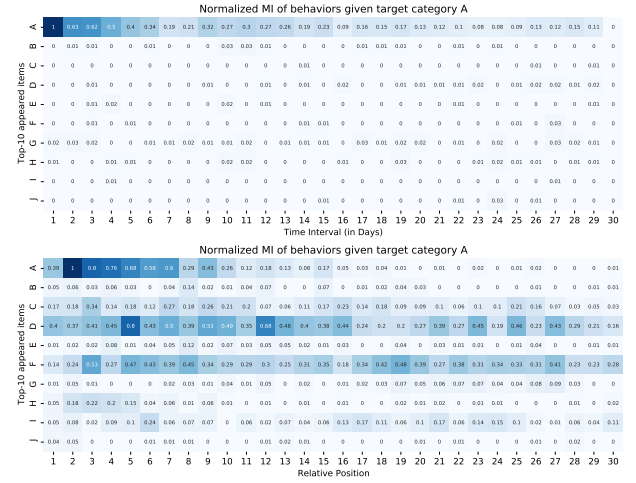


Figure 5: Semantic-temporal correlation on real-world datasets